



HAL
open science

A data driven approach using local measurements to locate turbine governors causing forced oscillations

Sigurd Hofsmo Jakobsen, Xavier Bombois, Santiago Sanchez Acevedo, Hallvar Haugdal, Salvatore D'arco

► To cite this version:

Sigurd Hofsmo Jakobsen, Xavier Bombois, Santiago Sanchez Acevedo, Hallvar Haugdal, Salvatore D'arco. A data driven approach using local measurements to locate turbine governors causing forced oscillations. 2023. hal-04191376

HAL Id: hal-04191376

<https://hal.science/hal-04191376>

Preprint submitted on 30 Aug 2023

HAL is a multi-disciplinary open access archive for the deposit and dissemination of scientific research documents, whether they are published or not. The documents may come from teaching and research institutions in France or abroad, or from public or private research centers.

L'archive ouverte pluridisciplinaire **HAL**, est destinée au dépôt et à la diffusion de documents scientifiques de niveau recherche, publiés ou non, émanant des établissements d'enseignement et de recherche français ou étrangers, des laboratoires publics ou privés.

A data driven approach using local measurements to locate turbine governors causing forced oscillations

Sigurd Hofsmo Jakobsen*, Xavier Bombois[†], Santiago Sanchez Acevedo*, Hallvar Haugdal*, Salvatore D'Arco*

* Sintef Energy Research Trondheim, Norway

[†]Laboratoire Ampère Ecole Centrale de Lyon, Université de Lyon, Ecully, France

Abstract—This paper presents a method to localize the source of forced oscillations due to power plant turbines and turbine governors based on model validation and system identification techniques. The method identifies the closed loop dynamics of power plants described by the swing equation. When forced oscillations are detected, they are located by finding the transfer functions that describe the behavior of the corresponding plants worse. The method presented in this paper locates the source of forced oscillations based only on local measurements at each plant. This may represent an inherent advantage since it may reduce the need of data measurement and communication. The performance is demonstrated by a n with an hardware-in-the-loop approach using a real time simulator and real phasor measurement units. Sensitivities of the method is analysed using a simulation tool.

Index Terms—System identification, forced oscillations, governor systems, power system dynamics.

I. INTRODUCTION

Low-frequency electro-mechanical oscillations in power systems can be categorized into natural oscillations and forced oscillations. Forced oscillations result from a malfunctioning component that introduces persisting periodic disturbances in the system. The progressive installation of phasor measurement units (PMUs) in the power system in the recent years led to an increased awareness and focus on forced oscillations since data analysis revealed their rather regular occurrence [1], [2].

If the forced oscillations coincide with poorly damped modes of the power system, amplification may occur resulting in threatening conditions for the power system operation even at relatively long distances from the source. Thus, the malfunctioning equipment causing the forced oscillation should be promptly localised and disconnected. When the oscillation amplitude is not amplified to constitute an imminent threat, forced oscillations can still be a symptom of a defective component that should be addressed. Despite that localizing the source of forced oscillations is a relevant issue for transmission system operators, this task is still very technically challenging.

This paper presents a method to localize the source of forced oscillations due to power plant governors based on model validation and system identification techniques. The idea behind the model validation based methods is that a

model explaining the behavior of a component during normal operation will fail to explain the behavior if the component is malfunctioning. One of the first model validation based methods [3] uses models of power system areas and PMU measurements from interface lines between different areas in the power system. The measurements are used as inputs to models of the areas in numerical simulations. The simulated area yielding the worst match with the measurements are flagged as the source for the forced oscillation.

Several methods for localising forced oscillations have been proposed in the literature [4]. A popular class of methods for localising the source of forced oscillations is represented by the energy based methods [5]–[10]. The key idea is to model the power system using energy functions and to assume that the component causing the forced oscillation is producing energy at the frequency of the forced oscillation. However, the most successful energy based approaches require not only local plant measurements, but also measurements of current and voltage at all power system buses. The approach presented in [11] localizes the source of forced oscillations assuming the knowledge of the susceptances of the branches adjacent to the generator buses and measurements of the electrical frequency at all generator buses and at their adjacent buses. Another recent method [12] uses a moving window fast Fourier transform for determining when a forced oscillation is first detected at different locations in the network followed by a triangulation scheme to find the source. The literature review [4] also mentions machine learning and statistical methods.

Several of the methods described in literature require an extensive amount of measurements geographically distributed in the power system. In this context, model validation methods may have less demanding requirements on measurements and data communication. Moreover, model validation based methods can offer an additional inherent advantage by ensuring correct and updated models for the dynamic components in the power system.

This paper applies system identification methods to identify a model of a power plant from measurements of electrical power and frequency obtained using a PMU. Similar methods that also uses system identification techniques have been proposed in [13], [14]. However, the method presented in [13] uses a system identification technique that may result in biased models as highlighted in [15]. The method presented in [14] is

This work was supported by the project SynchroPhasor-based Automatic Real-time Control (SPARC), funded by the ENERGIX Program of the Research Council of Norway, under Project 280967, and the industry partners, Statnett, Fingrid, Energinet, Svenska Kraftnät, Landsnet and GE.

purely data driven and does not offer a theoretical justification. The paper [16] uses methods from machine learning for identifying a model of a power plant but needs measurements of the derivative of the machines rotational speed in addition to the rotational speed and rotor angle. Although these quantities can be estimated from PMU measurements, it adds complexity and may reduce accuracy. Another model validation based method uses a model of an effective generator impedance that relates the voltage and current at generator bus bars [17]. A drawback of this method is that the obtained model does not represent a physical system.

In this paper we present a model based validation method that uses measurements local to each power plant. System identification is used to identify the transfer function representing the behavior of the plants during normal operation. When forced oscillations occur, the response of each power plant is compared to the response predicted by the corresponding previously identified transfer function. The power plant where the deviation between the predicted and observed response is largest is assumed to be the source of the forced oscillations. The concept/method is introduced in [15]. This paper extends this work by adding the following elements of novelty:

- A more detailed investigation of the effect of process noise on the identification, where the process noise could be vibrations in the turbine shaft or random fluctuations in the hydro power plant water ways.
- A more detailed and accurate evaluation of the difference between using frequency measurements and measurements of rotor angular speed for the method.
- A demonstration with a numerical example and a laboratory validation with an hardware in the loop approach using a real time simulator and real PMUs.

In Section II we present the mathematical models we assume in the paper. The method is presented in Section III. A laboratory validation is given in Section IV and an analysis of the method is given in Section V. Conclusions are given in Section VI.

II. MATHEMATICAL MODEL OF THE POWER SYSTEM

Our method relies on the identification of a model that can be deduced from measurements of the electrical power p_e and the rotor angular speed ω in a power plant using system identification techniques. Moreover, we will identify the model during normal operation, which means that the plant has to be sufficiently excited by an external signal that is statistically independent from any process noise in the plant. The identification procedure is already described in [18], [19], but we will also introduce the transfer function here and show that the dynamics of the power plants in a power system are inherently excited by external random load variations. The power plants, loads and how they are interconnected can be modelled as a set of stochastic differential algebraic equations

(SDAEs) [20]:

$$\begin{aligned}\dot{\mathbf{x}} &= \mathbf{f}(\mathbf{x}, \mathbf{y}, \boldsymbol{\eta}) \\ \mathbf{0} &= \mathbf{g}(\mathbf{x}, \mathbf{y}, \boldsymbol{\eta}) \\ \dot{\boldsymbol{\eta}} &= \boldsymbol{\alpha}(\mathbf{x}, \mathbf{y}, \boldsymbol{\eta}) + \mathbf{b}(\mathbf{y}, \boldsymbol{\eta})\boldsymbol{\zeta}\end{aligned}\quad (1)$$

where \mathbf{f} are the differential equations and \mathbf{g} are the algebraic equations. Moreover, \mathbf{x} are the state variables that include the rotational speed and the angle of synchronous machine rotors, and the dynamic states of loads and control systems while \mathbf{y} are the algebraic variables that include bus voltages and angles. The terms $\boldsymbol{\alpha}$ and \mathbf{b} are the drift and diffusion terms respectively of the stochastic perturbation $\boldsymbol{\eta}$, and $\boldsymbol{\zeta}$ is a vector of white noise.

To see which model we can identify using measurements of electrical power and electrical frequency we use the stochastic formulation of the swing equation from [20]:

$$\begin{aligned}\dot{\delta}(t) &= \omega(t) - \omega_s \\ \dot{\omega}(t) &= \frac{1}{M}(p_m(t) - p_e(t) - D(\omega(t) - \omega_s)) + \eta_\omega(t) \\ \dot{\eta}_\omega(t) &= \alpha_\omega(\mu_\omega - \eta_\omega(t)) + b_\omega\zeta_\omega(t)\end{aligned}\quad (2)$$

where δ is the rotor angle, ω_s is the synchronous speed, p_m is the mechanical power, M is the inertia constant of the plant, and D is the damping constant. The term η_ω represents a stochastic process that models rotor vibrations [20]. The process η_ω is parametrised by the mean μ_ω and the mean reversion rate α_ω while the variance is scaled with b_ω , and ζ_ω . We then linearise (2) and write it in the Laplace domain.

$$\Delta\omega(s) = G_J(s)(\Delta p_m(s) - \Delta p_e(s) + M\Delta\eta_\omega(s)) \quad (3)$$

with $G_J(s) = 1/(Ms + D)$. For the mechanical power $\Delta p_m(s)$ we assume the following linear relation:

$$\Delta p_m(s) = G_p(s)(r(s) - \Delta\omega(s)) = G_p(s)c(s) \quad (4)$$

where G_p includes the governor, servo and turbine dynamics of the plant, r is the reference for the speed and c is the input signal to the governor. We now substitute (4) into (3) with $r(s) = 0$

$$\Delta\omega(s) = G_0(s)(\Delta p_e(s) - M\Delta\eta_\omega(s)) \quad (5)$$

with

$$G_0(s) = -\frac{G_J(s)}{1 + G_J(s)G_p(s)} \quad (6)$$

From (5) we see that we can identify the transfer function G_0 described by (6) from measurements of the electrical power and rotational speed of a machine. It should be noted that due to the term $G_0M\Delta\eta_\omega$ in (5), we cannot fully represent $\Delta\omega$ with the transfer function G_0 and measurements of Δp_e . Moreover, the method can only localise forced oscillations caused by dynamics in G_0 , that is forced oscillations due to the governor, servo, or turbine.

To be able to identify the transfer function G_0 during normal operation, we need an external excitation. From (5) we see that the external excitation must be provided by the electrical

power p_e . We assume that this external excitation is provided by random load changes in the system. Moreover, we assume the loads to be described by the equations given in [20]:

$$\begin{aligned} p_L(t) &= (p_{L0} + \eta_p(t)) \left(\frac{v_L(t)}{v_{L,0}} \right)^\gamma \\ \dot{\eta}_p(t) &= \alpha_p(\mu_p - \eta_p(t)) + b_p \zeta_p(t) \end{aligned} \quad (7)$$

where $p_L(t)$, p_{L0} , $v_L(t)$ and $v_{L,0}$ are active power, and voltage at time t and at time $t = 0$ respectively. The constant part of the load models is consistent with standard load models where γ determines the share of constant power, current or impedance loads at a bus [21]. The parameters α_p , b_p , and μ_p are parameters for a Ornstein-Uhlenbeck process which is often a good choice for load modelling [22].

The random load changes influence the electrical power through the algebraic variables representing the voltage at generator terminals. This expression can conveniently be written using phasor notation:

$$p_e(t) = \Re\{3Y_d \vec{e}(t) \vec{v}_G^*(t)\} \quad (8)$$

where $\vec{e}(t)$ and $\vec{v}_G(t)$ are the phasors of the internal voltage and generator terminal voltage respectively, \vec{v}_G^* is the complex conjugate of \vec{v}_G and Y_d is the sub transient admittance of a power plant. If we assume Y_d to be purely reactive (8) simplifies to

$$p_e(t) = 3 \frac{|\vec{e}(t)| |\vec{v}_G(t)|}{X_d} \cos(\delta(t) - \theta(t)) \quad (9)$$

where θ is the angle of the phasor \vec{v}_G and $X_d = 1/Y_d$. The phasor \vec{v}_G varies stochastically due to the random load changes (7) and the process noise at power plants (3), thus power plants are externally excited. How the random load changes and process noises influence \vec{v}_G through the algebraic equations \mathbf{g} is shown in Appendix A.

In [18] it is pointed out that the estimate of G_0 may be biased if the process noise η_ω at a plant is too large. This is due to a direct coupling between the process noise and electrical power. This can more easily be seen if we linearise (9):

$$\begin{aligned} \Delta p_e(t) &= \left. \frac{\partial p_e}{\partial |\vec{e}|} \right|_{t=0} \Delta |\vec{e}(t)| + \left. \frac{\partial p_e}{\partial |\vec{v}_G|} \right|_{t=0} \Delta |\vec{v}_G(t)| \\ &+ \left. \frac{\partial p_e}{\partial \delta} \right|_{t=0} \Delta \delta(t) + \left. \frac{\partial p_e}{\partial \theta} \right|_{t=0} \Delta \theta(t) \\ &= K_e \Delta |\vec{e}(t)| + K_v \Delta |\vec{v}_g(t)| + K_\delta \Delta \delta(t) + K_\theta \Delta \theta(t) \end{aligned} \quad (10)$$

From (10) we see that the power plant will be externally excited by $\Delta |v_G|$ and $\Delta \theta$. In addition we see that the electrical power p_e of a plant will be directly influenced by the process noise η_ω through δ . However, it is reasonable to assume that the influence of $|v_G|$ and θ on p_e is significantly larger than the influence of η_ω , and thus we will still get a good estimate (see [18] for details).

To write (10) on a more compact form we group the parts of the internal voltage e that is a function of the rotational

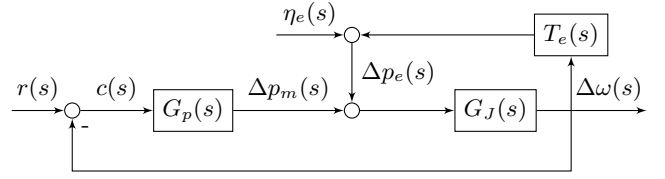


Fig. 1: Assumed model of a power plant in the power system

speed, due to the synchronisation torque, excitation system and power system stabiliser (PSS) together with $K_\delta \delta(s)$ into $T_e(s) \Delta \omega(s)$ while the rest of p_e we group into $\eta_e(s)$. With this we can depict the closed loop dynamics we want to identify as in Fig. 1, where we have omitted η_ω for simplicity. It should be note that forced oscillations caused by components in T_e will not be localised by our method.

III. MODEL VALIDATION METHOD DESCRIPTION

We will now present the method developed in [15] for localising the source of forced oscillations. First we write (5) in the discrete time domain for a power plant i and with some abuse of notation, we denote by z both the the shift operator and the Z-transform variable

$$\Delta \omega_i[n] = G_{0,i}(z) \Delta p_{e,i}[n] + \eta_i[n] \quad (11)$$

where $\eta_i[n]$ is the noise term $M G_0 \Delta \eta_{\omega,i}(s)$ in the discrete time domain and i in the subscript denotes generator i . We assume that during normal operation (i.e., when there is no forced oscillation), η_i can be modelled as a filtered white noise i.e., $\eta_i[n] = H_{0,i}(z) \zeta_{\omega,i}[n]$ for some discrete-time transfer function $H_{0,i}$. The Ornstein-Uhlenbeck process that can be seen as a low pass filtered white noise [23], hence the filtered noise assumption of η_i seems reasonable. It is important to stress that this process disturbance is statistically independent from the external excitation $\eta_{e,i}[n]$ corresponding to the random load changes (see Fig. 1)

Suppose now that a forced oscillation appears in one plant (say plant k) and that we model this forced oscillation as an extra sinusoidal disturbance at the output of the governor of this particular plant. In this case, the term η_k at plant k will also contain a sinusoidal term, while the term η_i in all the other plants will remain equal to filtered white noise. In fact, the forced oscillations at plant k will influence the other plants through the electrical power and will, therefore, not change the process disturbances at the other plants.

Based on the above reasoning, locating the source of the forced oscillation could be achieved by detecting a sinusoidal signal in the residual signal. For all $i \neq k$, we have:

$$\epsilon_i[n] = \Delta \omega_i[n] - G_{0,i}(z) \Delta p_{e,i}[n] = \eta_i[n] = H_{0,i}(z) \zeta_{\omega,i}[n] \quad (12)$$

while, at the plant k where the forced oscillation is present, we have

$$\begin{aligned} \epsilon_k[n] &= \Delta \omega_k[n] - G_{0,k}(z) \Delta p_{e,k}[n] \\ &= \eta_k[n] = H_{0,k}(z) \zeta_{\omega,k}[n] + A_k \sin(2\pi f_o t + \phi_k) \end{aligned} \quad (13)$$

where A_k , f_o , ϕ_k are respectively the amplitude, frequency and phase angle of the sinusoidal signal in the residual due to the forced oscillation.

This residual signal must be computed at each plant using measurements $\Delta\omega_i$ and $\Delta p_{e,i}$. If we knew $G_{0,i}$, we would have $\epsilon_i = \eta_i$ for all i . However, the true $G_{0,i}$ are all unknown and will be replaced in the computation of ϵ_i by the models G_i of $G_{0,i}$ identified during normal operation, using the system identification techniques developed in [18]. In short, we assume that, in normal operation (i.e., when there is no forced oscillation), the true system $G_{0,i}$ and $H_{0,i}$ for all i can be represented using the parameter vector $\theta_{0,i}$:

$$\Delta\omega_i[n] = G_{0,i}(z, \theta_{0,i})\Delta p_{e,i}[n] + H_{0,i}(z, \theta_{0,i})\zeta_{\omega,i}[n] \quad (14)$$

In the prediction error identification methodology, an estimate $\hat{\theta}_{N,i}$ of $\theta_{0,i}$ can be obtained using input-output data collected at power plant i and a model structure $\mathcal{M} = \{G_i(z, \theta_i), H_i(z, \theta_i)\}$ allowing to describe (14) (e.g., a so-called BJ model structure where the plant transfer function $G_i(z, \theta_i)$ and the noise transfer function $H_i(z, \theta_i)$ are parametrized independently). Note that prediction error identification is suited for data collected in open and in closed loop and achieves the minimum variance under Gaussian noise assumption [24]. The prediction error estimate $\hat{\theta}_{N,i}$ is given by:

$$\hat{\theta}_{N,i} = \arg \min_{\theta_i} \frac{1}{N} \sum_{n=1}^N (H_i^{-1}(z, \theta_i)(y_i[n] - G_i(z, \theta_i)u_i[n]))^2 \quad (15)$$

where $u_i[n]$ and $y_i[n]$ are $\Delta p_{e,i}[n]$ and $\Delta\omega_i[n]$ collected during normal operation and sampled to provide N samples of each.

Having obtained the parameter vector $\hat{\theta}_{N,i}$ using the prediction error criterion with data collected during normal operation, we can use the obtained models at a later stage with data collected at moments where a forced oscillation may have occurred to compute the residual signal:

$$\hat{\epsilon}_i[n] = \Delta\omega_i[n] - G_i(z, \hat{\theta}_{N,i})\Delta p_{e,i}[n] \quad (16)$$

The presence of a sinusoidal component in $\hat{\epsilon}_i$ can be detected by looking at the periodogram of $\hat{\epsilon}_i$. The fact that $G_i(z, \hat{\theta}_{N,i})$ is not precisely equal to $G_{0,i}(z, \theta_0)$ means that all $\hat{\epsilon}_i$ will contain some sinusoidal components, but the sinusoid at the plant where the forced oscillation is present will be the largest. Therefore, when a forced oscillation appears in the plant k , a large peak will appear in the periodogram of $\hat{\epsilon}_k$. It is also clear that the power of $\hat{\epsilon}_k$ will be increased with respect to normal operations.

The method can be summarised with the following sequence of steps:

- 1) Collect and preprocess data during normal operation. In this step it is good to collect as much data as possible. Half an hour of data should be more than sufficient based on past experience. The data should be filtered and decimated, more details can be found in [18] for details.

- 2) Use preprocessed data to estimate transfer functions.
- 3) Collect and preprocess data during forced oscillations. For this step one should collect enough data to at least capture a few cycles of the forced oscillation.
- 4) Calculate residuals using the transfer functions from step 2) and data from forced oscillation situations
- 5) Localise forced oscillations by finding the residual with the highest amplitude at the frequency of the forced oscillation.

The data can be collected using PMUs or control system data. It should be noted that when using PMUs we assume that frequency measured close to a generator is a good estimate for the rotational speed of its rotor. The preprocessing in step 1 and 3 consists of filtering, detrending and decimating the collected data.

IV. EXPERIMENTAL VALIDATION

The laboratory setup was configured as shown in Fig. 2, the connections in the figure show the links between an digital real time simulator (DiRTS) OPAL-RT, physical PMUs, and a phasor data concentrator (PDC). Additionally, an overview of the laboratory is shown in Figure 3. The N44 test system [25] depicted in Fig. 4 was implemented on the DiRTS an ABB PMU was placed on bus 5600 and a Siemens PMU on bus 6000. A PDC SEL 5073 was used to collect the PMUs voltages and currents. Loads are modelled as constant power loads with an added Wiener process that excites the dynamics of the power system. To add forced oscillations, a turbine and governor model was implemented in Modelica and exported as a co-simulation functional mock-up interface (FMI) with the possibility to add forced oscillations to the reference signal of the turbine governor. The amplitude used for the forced oscillations were 10 MW, which corresponds to around 1% [p.u.] for the machines tested. Due to storage and computational restrictions the sampling rate from the real time simulator was 0.2 s, this sampling rate also applies to the measurements we can get from the PMUs. The simulation time step was 2 ms.

For the identification we assumed a Box-Jenkins model structure and we collected data for half an hour. When localising the source of forced oscillations we collected data for 5 minutes. Although, as we show in the next section, good results can be obtained with significantly shorter time windows. In addition to the results from the PMUs we also give some results using rotational speed and electrical power from the DiRTS, in which case we also include results from bus 6100.

In Fig. 5 the periodograms of the electrical power calculated from the PMUs are depicted when there is a forced oscillation with a frequency of $0.2Hz$ applied to generator 1 at bus 5600. We see from the figure that there is no peak at $0.2Hz$. Similarly the periodogram of the electrical frequency from the PMUs are depicted in Fig. 6, where we also do not see the forced oscillation. This means that it is in this case is not possible to localise the source of the forced oscillation by only looking at the periodogram of the electrical power and frequency as measured at the terminal of the generator.

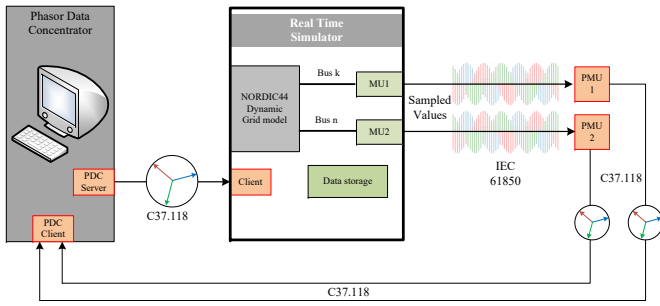


Fig. 2: Connections of laboratory setup.



Fig. 3: Laboratory setup. 1: Physical PMUs, 2: Real time simulator, 3: GPS clock and 4: Panoramic view of the laboratory.

In Fig. 7 the residuals obtained using our method and measurements from the rotational speed of the generators are depicted. We can clearly see that the periodogram of the residual for generator 1 at bus 5600 has a higher peak at 0.2 Hz than the other generators. The oscillation can also be clearly seen when plotting the residuals in the time domain as done in Fig. 8. In both Fig. 7 and Fig. 8 we have also included results from the generator at bus 6100 for comparison.

When using PMUs measurements it is not possible to distinguish between different generators at the same bus. This is due to the fact that the PMUs measure the voltage at the

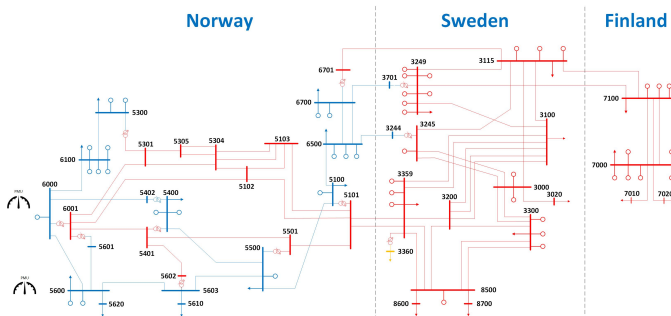


Fig. 4: Topology of the N44 test network

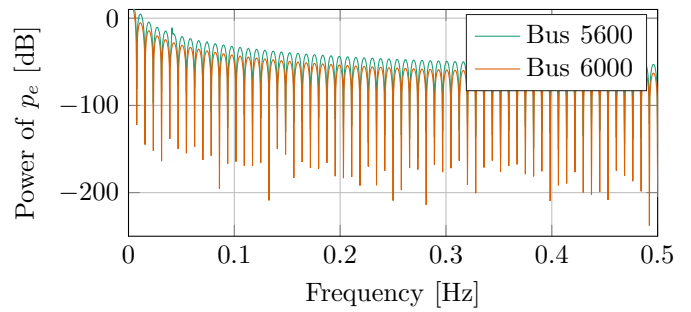


Fig. 5: Periodogram of electrical power calculated from PMUs when there is a forced oscillations at bus 5600 with a frequency of 0.2 Hz

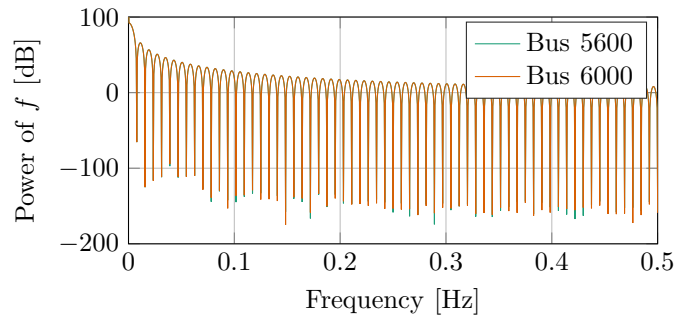


Fig. 6: Periodogram of frequency from PMUs when there is a forced oscillations at bus 5600 with a frequency of 0.2 Hz

bus and the currents flowing on the lines connected to the bus. The power is calculated from these measurements, and we can thus not calculate the power for each of the plants at the same bus separately. However, when looking at Figs. 9 and 10 we can clearly see that the oscillation is occurring at bus 5600, showing that the method also works for localising the source bus even if there are multiple generators connected to it. Results from bus 6100 is not included in this case since only two PMUs are connected to the system. In Fig. 11 we have plotted the results when applying a forced oscillation with a frequency of 0.3 Hz at bus 5600 and one with a frequency

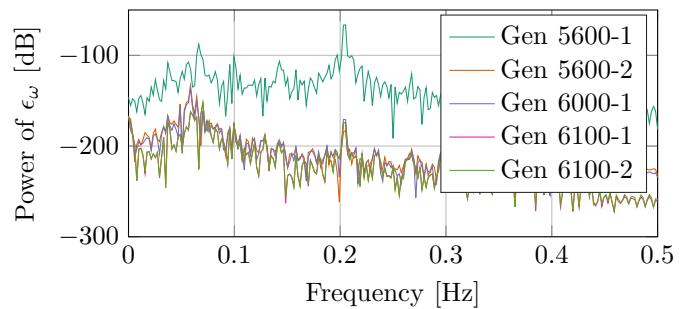


Fig. 7: Periodogram of residual using electric power and speed measurements from the DiRTS when there is a forced oscillations at bus 5600 with a frequency of 0.2 Hz

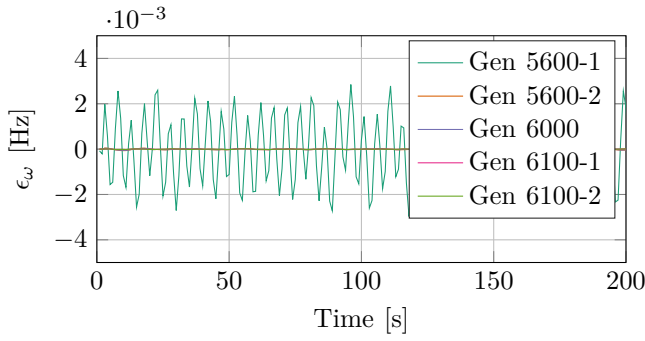


Fig. 8: Time domain plot of residual using electric power and speed measurements from the DiRTS when there is a forced oscillation at bus 5600 with a frequency of 0.2 Hz

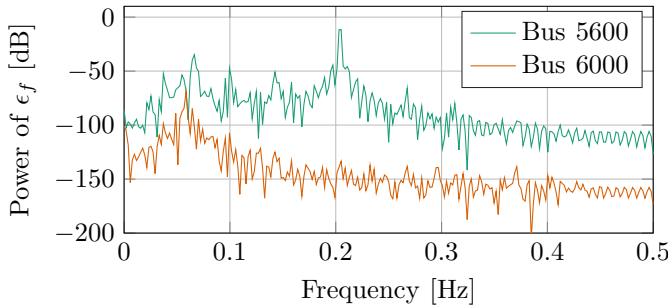


Fig. 9: Periodogram of residuals using pmu measurements when there is a forced oscillation at bus 5600 with a frequency of 0.2 Hz

of 0.2 Hz at bus 6000. From the figure we clearly see distinct peaks in the periodogram of the residual for the correct bus at the correct frequencies.

V. NUMERICAL RESULTS

In addition to the results using real PMUs we also validated the method using numerical simulation with DynPSSimPy [26]. We extended DynPSSimPy with a stochastic differential equations (SDE) solver based on the Euler-

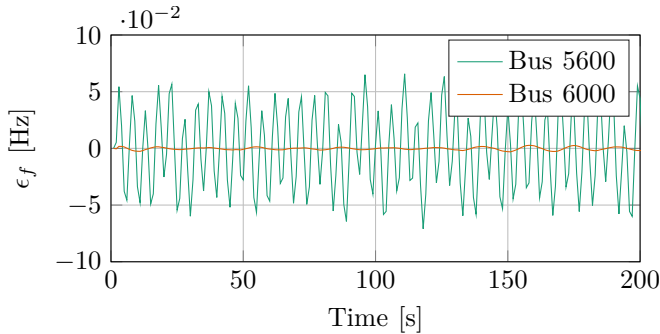


Fig. 10: Time domain plot of residual using PMUs measurements from the DiRTS when there is a forced oscillation with a frequency of 0.2 Hz at bus 5600.

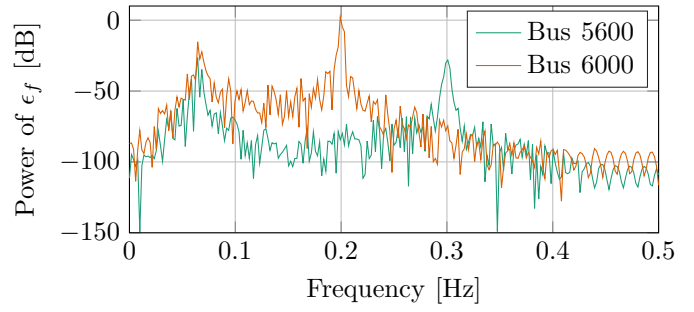


Fig. 11: Periodogram residual using PMU measurements real time simulation with forced oscillations with frequencies 0.3 Hz and 0.2 Hz at bus 5600 and 6000 respectively

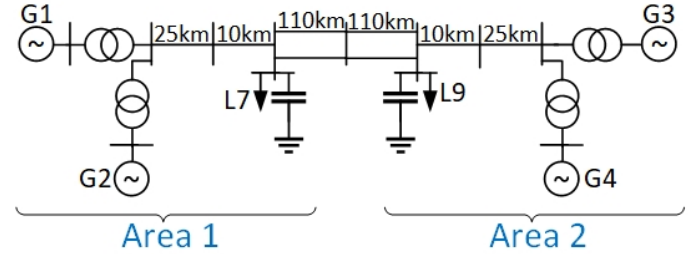


Fig. 12: Kundur two area system

Maruyama method was implemented with a time step of 5 ms. The loads were modelled as time varying admittances, which corresponds to (7) with $\gamma = 2$. Forced oscillations were introduced by applying a sinusoidal modulation of the speed reference of the governor with an amplitude of A_k and a frequency of f_o . For the test system we used the Kundur two area system [21] depicted in Fig. 12. Since the Nordic power system contains primarily hydro power, the power plants in the test system were replaced with the non-linear hydro governor model with the non-elastic water column described in [27].

We analysed the sensitivity of the method by running 100 times all possible combinations of the parameter combinations listed below.

- Process noise levels $b_\omega \in \{10^{-5}, 10^{-4}\}$ for details see (2).
- Forced oscillations amplitudes $A_k \in \{0.1\%, 1\%\}$ of 50 Hz.
- Ten forced oscillations with frequencies linearly spaced from 0.1 Hz to 1.9 Hz.
- Forced oscillation at each of the generators

This resulted in 16000 stochastically independent cases. The amplitude of the stochastic load variation was selected such that the frequency variation stayed within 0.01 Hz. An often used assumption is that power system frequency measured close to a generator is a good estimate for the generators' rotational speed $\Delta\omega \approx \Delta f$. We checked this assumption by using both measurements of the generators' rotational speed and the electrical frequency at the generator bus bars for the cases described above. Since DynPSSimPy uses phasor

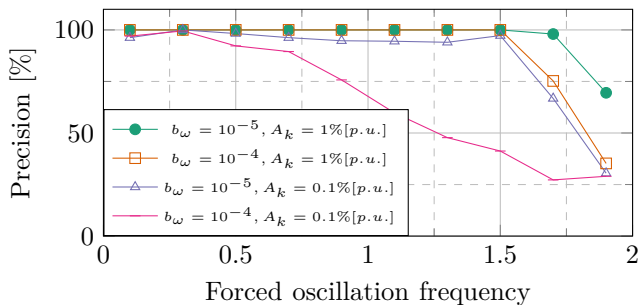


Fig. 13: Percentage correct localisation as a function of the forced oscillation frequency using rotational speed and electrical power for the identification

simulation we had to estimate the frequency from the voltage angle at the generator buses. This was done using a phased locked loop (PLL).

For the identification we used a Box-Jenkins model structure and a sampling rate of 4 Hz and one hour of data. With higher sampling rates it was difficult to get good models when using measurements of electrical frequency instead of rotational speed. When localising the source of forced oscillations we collected data for 20 seconds, which would give us two periods for the slowest forced oscillation we tested.

In Fig 13 we have plotted the percentage of correct localisation as a function of the frequency of the forced oscillation with different simulation parameters kept constant. We see that in all cases the performance drops as the frequency of the forced oscillations approaches the Nyquist frequency of $2Hz$. We see that in the best case with $b_\omega = 10^{-5}$ and $A_k = 1\% [p.u.]$ we have a 100% correct localisation until 1.5 Hz, but it does not drop much until 1.9 Hz. In the second case we increase the amplitude of the process noise to $b_\omega = 10^{-4}$, the localisation is still perfect up to 1.5 Hz, but the performance decreases more sharply than in the best case. With the process noise of $b_\omega = 10^{-5}$ and a forced oscillation amplitude of $A_k = 0.1\% [p.u.]$ we see that the performance is slightly below 100% for most of the frequencies except for the faster frequencies where the performance is worse. In the worst scenario when the process noise is $b_\omega = 10^{-4}$ and the forced oscillation amplitude $A_k = 0.1\% [p.u.]$ we see that the performance is significantly reduced. In Fig. 14 we have plotted the same as in Fig. 13, but with frequency instead of rotational speed. From the figure we see that the performance when using frequency instead of rotational speed is quite similar.

VI. CONCLUSIONS

In this paper we have demonstrated that it is possible to localise the source of a forced oscillation due to governor dynamics using system identification technique and model validation techniques. The method is demonstrated both using commercially available PMUs and in simulations. The method can localise multiple sources of forced oscillations simultaneously and also localise the correct bus when multiple

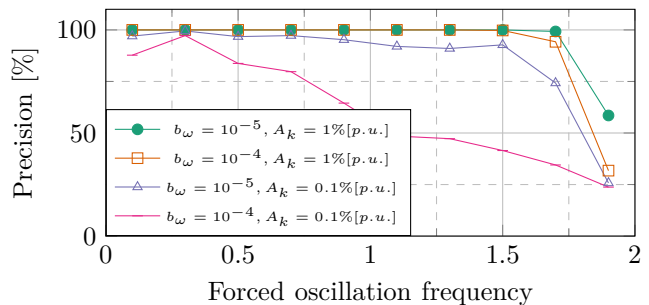


Fig. 14: Percentage correct localisation as a function of the forced oscillation frequency using electrical frequency and electrical power for the identification

generators are connected to the same bus. Although the method assumes measurements of rotational speed and electrical power, both the experimental and numerical validation show that the method performs well with measurements of electrical frequency instead of rotational speed.

A sensitivity analysis shows that the method works well for all frequencies of the forced oscillation up to close to the Nyquist frequency for the identified model. When using frequency measurements we managed to get good models with a sampling rate up to 4 Hz, which gives a Nyquist frequency of 2 Hz. This means that the method is applicable for forced oscillations with a frequency slightly below 2 Hz. It should be noted that the dynamics of faster controllers such as automatic voltage regulators (AVRs) and PSSs are not included in the identified models, other methods should therefore be used for forced oscillations caused by such components. The sensitivity analysis also shows that the method performs well for small amplitudes of the forced oscillation. The method also works well with relatively large process noise. We assume that the process noise models stochastic processes in the plant such as random vibrations in the rotor shaft. We do not know the magnitude of this process noise, but it is most likely present. The sensitivity analysis reveals that if both the amplitude of the forced oscillation is low 0.1 % of 50 Hz at the input to the turbine governor and the process noise level is high the performance of the method is poor. To our knowledge most other papers proposing data based model validation for localising the source of forced oscillations have not considered this process noise. Several of these methods should therefore be further investigated under the presence of process noise.

APPENDIX A STOCHASTICITY OF v_G

We will here show that the terminal voltage v_g varies stochastically for all power plants. For simplicity we will use phasor notation and drop the time dependence from the rest of calculations. To show how the stochastic loads described by (7) perturb the power plants, we will solve the algebraic equations \mathbf{g} using the current injection model

$$\vec{i}_{inj} = \vec{Y} \vec{v} \quad (17)$$

Where \vec{i}_{inj} is the Norton current of the dynamic components in the power system. \vec{Y} is the admittance matrix of the system including the generator and load admittances, $\vec{v} = [\vec{v}_G \ \vec{v}_L]^T$ are all the bus voltages in the system where \vec{v}_G and \vec{v}_L are the generator terminal and load voltages respectively. To simplify we assume that $\gamma = 2$ in (7). This means that we can write:

$$\vec{i}_{inj} = \begin{bmatrix} \vec{i}_G \\ \vec{0} \end{bmatrix} \quad (18)$$

with (18) we can rewrite (17) as:

$$\begin{bmatrix} \vec{i}_g \\ \vec{0} \end{bmatrix} = \begin{bmatrix} \vec{Y}_{GG} & \vec{Y}_{GL} \\ \vec{Y}_{LG} & \vec{Y}_{LL} \end{bmatrix} \begin{bmatrix} \vec{v}_G \\ \vec{v}_L \end{bmatrix} \quad (19)$$

As is pointed out in [28] we can now eliminate \vec{v}_L from (19) and introduce the reduced admittance matrix:

$$\vec{Y}_r = \vec{Y}_{GG} - \vec{Y}_{GL}\vec{Y}_{LL}^{-1}\vec{Y}_{LG} \quad (20)$$

with this (19) can be written as:

$$\vec{i}_G = \vec{Y}_r \vec{v}_G \quad (21)$$

\vec{i}_G is the Norton current of the electrical machines, that is:

$$\vec{i}_G = \vec{Y}_G \vec{e} \quad (22)$$

Where \vec{Y}_g is a diagonal matrix with the generator admittances. We can now write the generator terminal voltages as:

$$\vec{v}_G = \vec{Y}_r^{-1} \vec{Y}_G \vec{e} \quad (23)$$

REFERENCES

- [1] M. Ghorbaniparvar, "Survey on forced oscillations in power system," *Journal of Modern Power Systems and Clean Energy*, vol. 5, no. 5, pp. 671–682, Sep. 1, 2017, ISSN: 2196-5420.
- [2] H. Ye, Y. Liu, P. Zhang, and Z. Du, "Analysis and detection of forced oscillation in power system," *IEEE Transactions on Power Systems*, vol. 32, no. 2, pp. 1149–1160, 2016.
- [3] J. Ma, P. Zhang, H.-j. Fu, B. Bo, and Z.-y. Dong, "Application of Phasor Measurement Unit on Locating Disturbance Source for Low-Frequency Oscillation," *IEEE Transactions on Smart Grid*, vol. 1, no. 3, pp. 340–346, Dec. 2010, ISSN: 1949-3061.
- [4] T. Surinkaew, K. Emami, R. Shah, S. Islam, and N. Mithulananthan, "Forced Oscillation in Power Systems With Converter Controlled-Based Resources—A Survey With Case Studies," *IEEE Access*, vol. 9, pp. 150 911–150 924, 2021, ISSN: 2169-3536.
- [5] Y. Yu, Y. Min, L. Chen, and P. Ju, "The disturbance source identification of forced power oscillation caused by continuous cyclical load," in *2011 4th International Conference on Electric Utility Deregulation and Restructuring and Power Technologies (DRPT)*, Jul. 2011, pp. 308–313.
- [6] L. Ying, S. Chen, and L. Feng, "An energy-based methodology for locating the source of forced oscillations in power systems," in *2012 IEEE International Conference on Power System Technology (POWERCON)*, Oct. 2012, pp. 1–6.
- [7] L. Chen, Y. Min, and W. Hu, "An energy-based method for location of power system oscillation source," *IEEE Transactions on Power Systems*, vol. 28, no. 2, pp. 828–836, May 2013, ISSN: 1558-0679.
- [8] S. Maslennikov, B. Wang, and E. Litvinov, "Dissipating energy flow method for locating the source of sustained oscillations," *International Journal of Electrical Power & Energy Systems*, vol. 88, pp. 55–62, Jun. 1, 2017, ISSN: 0142-0615.
- [9] S. Feng, B. Zheng, P. Jiang, and J. Lei, "A Two-Level Forced Oscillations Source Location Method Based on Phasor and Energy Analysis," *IEEE Access*, vol. 6, pp. 44 318–44 327, 2018, ISSN: 2169-3536.

- [10] I. Singh, V. K. Reddy Chiluka, D. J. Trudnowski, and M. Donnelly, "A Strategy for Oscillation Source Location Using Closed-Contour Grouping and Energy-Flow Spectra," in *2020 IEEE/PES Transmission and Distribution Conference and Exposition (T D)*, Oct. 2020, pp. 1–5.
- [11] A. Ortega and F. Milano, "Source Location of Forced Oscillations based on Bus Frequency Measurements," in *2021 IEEE 30th International Symposium on Industrial Electronics (ISIE)*, Jun. 2021, pp. 01–06.
- [12] W. Wang, C. Chen, L. Zhu, *et al.*, "Model-less Source Location for Forced Oscillation based on Synchrophasor and Moving Fast Fourier Transformation," in *2020 IEEE PES Innovative Smart Grid Technologies Europe (ISGT-Europe)*, Oct. 2020, pp. 404–408.
- [13] R. Xie and D. Trudnowski, "Comparison of methods for locating and quantifying turbine-induced forced-oscillations," in *2017 IEEE Power Energy Society General Meeting*, Jul. 2017, pp. 1–5.
- [14] T. D. Duong and S. D'Arco, "Locating Generators Causing Forced Oscillations Based on System Identification Techniques," in *2020 IEEE PES Innovative Smart Grid Technologies Europe (ISGT-Europe)*, Oct. 2020, pp. 191–195.
- [15] S. H. Jakobsen, X. Bombois, and S. D'Arco, "Data-based model validation for locating the source of forced oscillations due to power plant governors," in *2022 International Conference on Smart Energy Systems and Technologies (SEST)*, Sep. 2022, pp. 1–6.
- [16] Y. Cai, X. Wang, G. Joós, and I. Kamwa, "An Online Data-Driven Method to Locate Forced Oscillation Sources From Power Plants Based on Sparse Identification of Nonlinear Dynamics (SINDY)," *IEEE Transactions on Power Systems*, vol. 38, no. 3, pp. 2085–2099, May 2023, ISSN: 1558-0679.
- [17] S. C. Chevalier, P. Vorobev, and K. Turitsyn, "Using Effective Generator Impedance for Forced Oscillation Source Location," *IEEE Transactions on Power Systems*, vol. 33, no. 6, pp. 6264–6277, Nov. 2018, ISSN: 1558-0679.
- [18] S. H. Jakobsen, X. Bombois, and K. Uhlen, "Non-intrusive identification of hydro power plants' dynamics using control system measurements," *International Journal of Electrical Power & Energy Systems*, vol. 122, p. 106 180, Nov. 1, 2020, ISSN: 0142-0615.
- [19] S. H. Jakobsen, K. Uhlen, and X. Bombois, "Identification of hydro turbine governors using PMU data," in *2018 IEEE International Conference on Probabilistic Methods Applied to Power Systems (PMAPS)*, Jun. 2018, pp. 1–6.
- [20] F. Milano and R. Zárate-Miñano, "A Systematic Method to Model Power Systems as Stochastic Differential Algebraic Equations," *IEEE Transactions on Power Systems*, vol. 28, no. 4, pp. 4537–4544, Nov. 2013, ISSN: 1558-0679.
- [21] P. Kundur, N. J. Balu, and M. G. Lauby, *Power System Stability and Control*. McGraw-hill New York, 1994, vol. 7.
- [22] C. Roberts, E. M. Stewart, and F. Milano, "Validation of the Ornstein-Uhlenbeck process for load modeling based on μ PMU measurements," in *2016 Power Systems Computation Conference (PSCC)*, Jun. 2016, pp. 1–7.
- [23] E. Bibbona, G. Panfilo, and P. Tavella, "The Ornstein-Uhlenbeck process as a model of a low pass filtered white noise," *Metrologia*, vol. 45, no. 6, S117, Dec. 2008, ISSN: 0026-1394.
- [24] L. Ljung, *System Identification: Theory for the User*, second. United States of America: Prentice Hall, 1998.
- [25] L. Vanfretti, L. Dosiek, J. W. Pierre, *et al.*, "Application of ambient analysis techniques for the estimation of electromechanical oscillations from measured PMU data in four different power systems," *European Transactions on Electrical Power*, vol. 21, no. 4, pp. 1640–1656, 2011, ISSN: 1546-3109.
- [26] H. Haugdal and K. Uhlen, "An Open Source Power System Simulator in Python for Efficient Prototyping of WAMPAC Applications." arXiv: 2101.02937. (Jan. 8, 2021), [Online]. Available: <http://arxiv.org/abs/2101.02937> (visited on 05/10/2023), preprint.
- [27] Working Group on Prime Mover and Energy Supply Models for System Dynamic Performance Studies, "Hydraulic turbine and turbine control models for system dynamic studies," *IEEE Transactions on Power Systems*, vol. 7, no. 1, pp. 167–179, Feb. 1992, ISSN: 0885-8950.
- [28] F. Milano, *Power System Modelling and Scripting*. Springer Science & Business Media, 2010, ISBN: 978-3-642-13668-9.